Applied Energy 359 (2024) 122752

Contents lists available at ScienceDirect

Applied Energy

journal homepage: www.elsevier.com/locate/apenergy

A hybrid method based on logic predictive controller for flexible hybrid microgrid with plug-and-play capabilities

Muhammed Cavus [a,b,*], Adib Allahham [c], Kabita Adhikari [a], Damian Giaouris [a]

[a] School of Engineering, Newcastle University, NE1 7RU, UK
[b] School of Engineering, Iskenderun Technical University, 31200, Turkey
[c] Faculty of Engineering and Environment, Northumbria University, NE1 8ST, UK

GRAPHICAL ABSTRACT

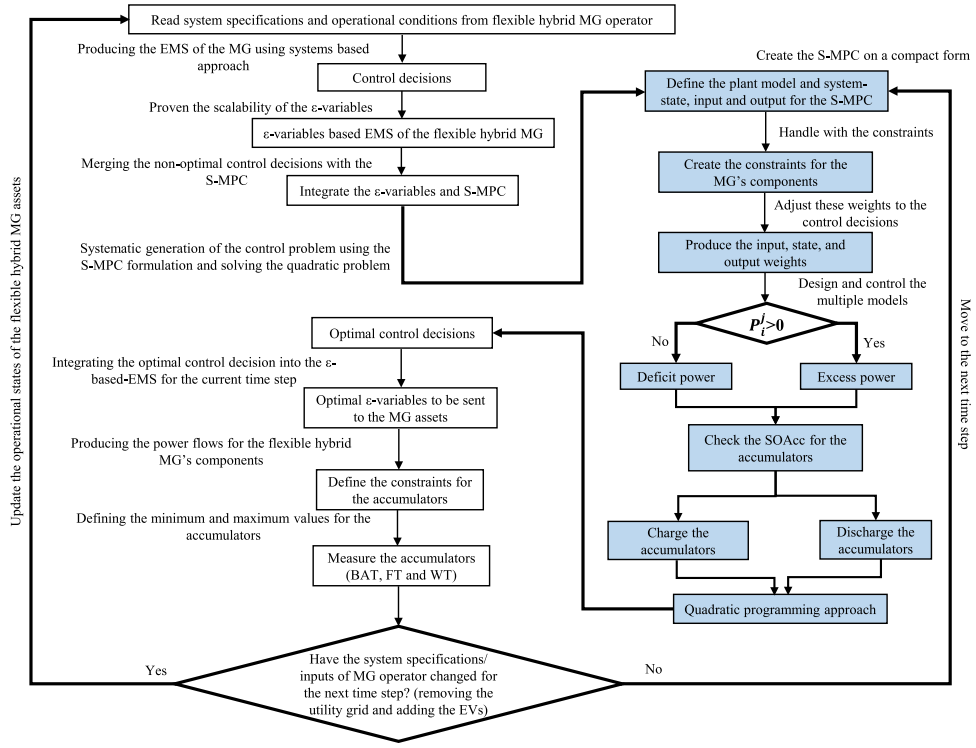

ARTICLE INFO

Keywords:
Control and optimization
Energy management
ε-variables
Logical control

ABSTRACT

Controlling flexible hybrid microgrids (MGs) is difficult due to the system's complexity, which includes multiple energy sources, storage devices, and loads. Although adding new components to the MG system through the plug-and-play (PnP) feature enables operating of the system in different modes, it adds to the system's complexity, hence necessitates careful control system design. The most challenging aspect of designing the

* Corresponding author at: School of Engineering, Newcastle University, NE1 7RU, UK.
E-mail address: m.cavus2@newcastle.ac.uk (M. Cavus).

https://doi.org/10.1016/j.apenergy.2024.122752
Received 18 September 2023; Received in revised form 29 December 2023; Accepted 23 January 2024
Available online 31 January 2024
0306-2619/© 2024 The Author(s). Published by Elsevier Ltd. This is an open access article under the CC BY license (http://creativecommons.org/licenses/by/4.0/).

Microgrid
Switched model predictive control

control system is ensuring that it can control the MG optimally in its various modes of operation. Previous methods based on logical control allow for synthesizing a controller capable of controlling the MG in its various operational modes. However, the resultant controller does not optimally operate the MG. Classical model predictive control allows optimal control of the MG only in specific operating modes. On the other hand, switched model predictive control (S-MPC) can optimally control the MG in its various modes. However, the design of S-MPC is complex, particularly for MGs with many operating modes or complex switching logic. Multiple factors contribute to the complexity, including model development, mode detection, and switching logic. This paper presents a hybrid method based on ε-variables and classical MPC for constructing the S-MPC for flexible hybrid MG with PnP capabilities. Our results show that the proposed controller synthesis approach provides an effective solution for optimally controlling flexible hybrid MGs with PnP capabilities as the proposed method enables: (i) an increase in the amount of energy export to the utility grid by 50.77% and (ii) a significant decrease in the amount of energy import from the grid by 46.7%.

1. Introduction

A hybrid flexible microgrid (MG) is a small-scale power system that integrates and manages multiple energy sources, including renewable energy sources (RESs) such as solar, wind, and hydro, as well as conventional sources such as diesel generators [1,2]. MG is designed to operate either connected or disconnected from the main power grid, providing a reliable and sustainable power supply for various applications [3,4]. The flexibility of a MG refers to the MG's capability to vary energy demand and its ability to optimize the available energy sources [5,6].

Adding the plug-and-play (PnP) capability to the MG's assets facilitates the system's installation and operation. PnP assets can enhance the MG's flexibility [7]. For instance, incorporating PnP electric vehicles (EVs) into a MG can increase the MG's flexibility [8,9] by varying the size of available storage capacity dynamically. PnP EVs can be added or removed from the MG system without extensive reconfiguration [10]. However, having assets with PnP capabilities makes the MG operate in multiple operational modes. This makes the design of optimal control of the MG challenging.

1.1. Literature review

Model Predictive Control (MPC) is widely used in the literature to control MGs [11,12]. A rolling horizon approach is applied in [13] to reduce the operational cost of the MG and to maximize the income from exporting power to the utility grid. A scenario-based MPC is presented in [14] with an objective to reduce carbon emission. The authors in [15] used the interval predictions to reduce the impact of the uncertainty in renewable energy generation, which, in its turn, reduced the operational cost significantly. To reduce the impact of uncertainty of energy demand and renewable energy generation, a robust MPC (R-MPC) was developed in [16]. A robust rolling-horizon MPC is presented in [17,18] to control in real time a community of buildings, which are represented as MGs. The control philosophy in [17,18] improves the robustness of the residential MGs in the face of real-time weather and energy price prediction errors. [19] presents a distributed MPC-based energy scheduling problem for multi-island microgrids. Through energy coordination, the objective is to achieve supply–demand equilibrium in an individual MG and reduce battery degradation for its extended cycle life. To solve the MPC optimization problem, a mixed-integer quadratic programming strategy is utilized [20]. [21] proposes a multiple-time-scale energy management solution for a hydrogen-based multi-energy MG to supply electricity, hydrogen, and heating loads, to minimize the multi-energy MG operational cost. The proposed solution consists of day-ahead energy scheduling and MPC-based real-time energy dispatch. The numerical results demonstrate that the proposed solution outperforms the benchmark solution, with mean daily operational costs 37.08% less than the benchmark solution.

It is important to notice that all these MPC methods are able to control the MG only in one operational mode, allow it to meet different objectives in this operational mode, and are able to consider the impact of the uncertainty of renewable generation and energy demand. These methods do not allow for control of the MG with different operational modes. On the other hand, many methods are developed to control complex systems with different operational modes. These methods are based on system state and use Petri Nets [22] and/or automata [23–26]. Other methods are based on the evolution/logical operators and the states graph [27,28]. The authors in [27,28] used the ε-variables to define the system evolution and the system graph to model the operational states/modes of the energy system. The mutual use of graph theory and the evolution operators presented in [27,28] allows us to address the problem of system scalability, and this is by considering all the possible operational modes of the system assets in the system graph. It is important to highlight that the PnP feature of the system's assets will change the system's size dynamically. This means the MG controller must deal with the scalability issue. The main drawback of these methods is that the resultant controller does not operate the MG in its different operational modes optimally.

Switched Model Predictive Control (S-MPC) is a variation of MPC that employs multiple models, each representing a distinct mode of system operation. S-MPC chooses the appropriate model and associated optimal control strategy based on the current state of the system and the system objectives. This enables S-MPC to deal with systems with mode-dependent dynamics. The main difference between MPC and S-MPC is that MPC uses a single model to control the system [29]; however, S-MPC uses multiple models and switches between them according to the current state of the system [30,31]. The authors in [30,31] demonstrated the development S-MPC to control a MG.

It is important to highlight that the construction of S-MPC is challenging, especially for MG with a large number of operational modes. The challenge arises from the following factors:

- S-MPC development requires the development of multiple models that represent the system's behavior in the different operational modes. In addition, the MG can have different objectives; in each operational mode, the MG can have an objective that is different from the objective in the other operational modes.
- S-MPC development requires the design of switching logic that maps the current state of the system to the appropriate model and the switching conditions between the operational modes.

Dealing with these challenges requires an exhaustive knowledge of the system and its desired behavior in each operational mode. Putting all the knowledge together to build the S-MPC must be done in a systematic way.

1.2. Contributions and research questions

Controlling the flexible hybrid MG in which the assets have PnP capabilities requires building a controller which is able to consider all the possible operating modes of the MG. The classical model predictive controller allows to control of the MG optimally in a specific operational mode but cannot represent the different possible operational modes. On the other hand, the control methods based on the mutual use of graph theory and the evolution operators can control the MG in its different operational modes, but the resultant operation of the MG is

Nomenclature

Δt	Time interval, 1 h
η_{ch}^{l}	Charging efficiency of accumulator l
η_{dis}^{l}	Discharging efficiency of accumulator l
$\mu, \gamma, \overline{\mu}, \overline{\gamma}$	Constraints in compact form
Φ	Evolution operator
$\varepsilon_{a\to b}(k)$	Binary variable that describes the state of connection between nodes a and b
ε_{EL}	Final evolution operator of EL
ε_{FC}	Final evolution operator of FC
ε_i	State of converter i
ε_i^{Avl}	Boolean variable that determines the availability of using converter i
ε_i^{Gen}	Generic condition for converter i
ε_i^{Req}	Boolean variable that determines the requirement of using converter i
A, B	Coefficients of MPC
BAT	Battery
C	Control weight
$C_{EV_{1,2,3}}^{max}(k)$	Maximum battery capacities for EV_1, EV_2 and EV_3
C_l	Capacities of accumulator l, [kWh]
EL	Electrolyzer
EV	Electric Vehicle
EV_{LD}	Power flow from the EV to the LD
F	Faraday constant
$F_{a\to b}^{j}(k)$	Flow of j from node a to node b
F_{EL}	amount of active power in EL [kW]
F_{FC}	amount of active power in FC [kW]
$F_{in\_BAT_{Power}}$	Total power in the BAT
$F_{in\_FT_{H_2}}$	Flow of hydrogen from the FT to the FC
$F_{in\_WT_{H_2O}}$	Flow of water from the WT to the EL
$F_{out\_BAT_{Power}}$	Power from the BAT to the EL
$F_{out\_EL_{H_2}}$	Flow of hydrogen from the EL to the FT
$F_{out\_FC_{H_2O}}$	Flow of water from the FC to the WT
$F_{out\_FC_{H_2O}}$	Flow of water to the FC
$F_{out\_FC_{H_2}}$	Flow of hydrogen to FC
$F_{out\_FC_{Power}}$	Power flow to the FC
$F_{out\_FC_{Power}}$	Power from the FC to the BAT
$F_{out\_FT_{H_2}}$	Flow of hydrogen from FT to the EL
F_{out_GR}	Power output in the GR
$F_{out\_GR_{Power}}$	Power for the LD
F_{out_PV}	Power output in the PV
$F_{out\_PV_{Power}}$	Power for the LD, BAT, and GR.
$F_{out\_WT_{H_2O}}$	Flow of water from the WT to the EL
FC	Fuel cell
$Flows$	Set of flows
FT	Fuel Tank
G, H, X	Parameters for quadratic problem
GR	Grid
H_2	Hydrogen
H_2O	Water
I_{elec}	Operating current for the EL
I_{FC}	Operating current for the FC
J_1, J_2, J_3	Cost functions
L	Logical Operator, [AND/OR]
L^{Av}	Logical operator for availability
L^{Gen}	Logical operator for general condition
L^{Req}	Logical operator for requirement
LD	Load
N	Horizon of the quadratic problem
$n_{c_{FC}}$	The number of cells for the FC
N_c	Control horizon, 24h
n_c	The number of cells for the EL
n_e	The number of electrons
n_F	Faraday's efficiency
n_{H_2O}	The generation rate of H_2O in the FC
n_{H_2}	The generation rate of H_2 in the EL
N_p	Prediction horizon, 24 h
P_{10}, FC_{WT}	Flow of water from the FC to the WT
P_{11}, WT_{EL}	Flow of water from the WT to the EL
P_1, GR_{LD}	Power flow from the GR to the LD
P_2, PV_{LD}	Power flow from the PV to the LD
P_3, PV_{GR}	Power flow from the PV to the GR
P_4, PV_{BAT}	Power flow from the PV to the BAT
P_5, BAT_{LD}	Power flow from the BAT to the LD
P_6, FC_{BAT}	Power flow from the FC to the BAT
P_7, BAT_{EL}	Power flow from the BAT to the EL
P_8, EL_{FT}	Flow of hydrogen from the EL to the FT
P_9, FT_{FC}	Flow of hydrogen from the FT to the FC
P_i^j	Power of j from node a to node b
P_{LD}	Load demand data
P_m	Power flows, $m = 1, 2, \cdots, 11$
P_m^{max}	Maximum values of power flows, 5 kW
$P_{net}(k)$	Differences between energy generation and consumption
P_{PV}	PV data
PV	Photovoltaic
Q	State weight
Q_f	Final cost weight
$R(k)$	Reference matrix
Rs^{Acc}	Set of accumulators
Rs^{Con}	Set of converters
s	State of microgrid
$SOAcc^l(1)$	Initial value of state of accumulator l
$SOAcc^l$	State of accumulator l
$SOAcc_{max}^l$	Maximum value state of accumulator l
$SOAcc_{min}^l$	Minimum value state of accumulator l
$str_{a\to b}^{SOAcc^l}$	Starting value of hysteresis zone of accumulator i for the connection a to b
$U(k)$	Optimal input vector
$u(k)$	System-input (control) vector
w_1, w_2, w_3, w_4, w_5	Positive weight coefficient
WT	Water tank
$x(k)$	System-state vector
$x_{a_1}, x_{a_2}, x_{a_3}$	Parts of system-state vector
$Y(k)$	Optimal output vector
$y(k)$	System-output vector
y_a, y_b, y_c, y_d, y_e	Parts of system-output vector
EMS	Energy Management Strategy
ESS	Energy Storage System
MG	Microgrid

MPC	Model Predictive Control
PnP	Plug-and-Play
QP	Quadratic Programming
R-MPC	Robust Model Predictive Control
RES	Renewable Energy Source
S-MPC	Switched Model Predictive Control
TP	Transition point

not optimal. S-MPC can control the MG optimally in its different operational modes; however, the construction of this controller is complex and requires a strong knowledge of the system and its desired behavior in each operational mode. The complexity of the S-MPC arises from the need to put all this knowledge to produce the final S-MPC. The main contribution of this paper is to present a systematic method to build the switched model predictive controller of a flexible hybrid MG with PnP assets. This method is based on combining logical control, graph theory, and classical MPC. The main contributions of this paper are as follows:

- The system graph and the evolution parameters allow us to define the operational modes, the switching conditions, and the state variables in each operational mode.
- The classical MPC allows us to find the optimal control decisions in each operational mode according to the objective defined for each operational mode.

Based on the method of controller synthesis proposed in this paper, the following research questions can be addressed:

- The paper suggests an approach for systematically generating S-MPC to regulate flexible hybrid Microgrids (MGs), taking into account the Plug and Play (PnP) capabilities of assets.
- The methodology proposed in this paper outlines a systematic process for generating S-MPC tailored for the control of flexible hybrid MGs, particularly those equipped with Plug and Play (PnP) capabilities in their assets.
- The paper also delves into the practical implementation of decisions derived from S-MPC in a simplified manner, contributing to the feasibility of applying these decisions effectively.

1.3. Organization of this paper

The rest of the paper is organized as follows: Section 2 shows the motivation of the paper. Section 3 presents the methodology of the hybrid method based on controlling flexible MG with PnP capabilities. Section 4 illustrates a detailed description of the hybrid method implementation. The simulation results of four case studies with the hybrid method based on controlling flexible MG are discussed in Section 5. Finally, Section 6 outlines the conclusions and addresses future work.

2. Motivation

The development of advanced control systems for microgrids (MGs) has been the focus of extensive research due to their potential to enhance energy management, improve grid resilience, and facilitate the integration of renewable energy sources. Existing MG control methods, such as logic-based control and MPC, offer valuable solutions, yet they face certain limitations in addressing the complex operational scenarios of flexible MGs with PnP capabilities.

Flexible MGs with PnP capabilities, characterized by diverse energy resources and the dynamic integration of PnP assets such as EVs, present unique challenges that require innovative control strategies. The state of the art in MG control often lacks a systematic approach to seamlessly adapt to these complexities, making it essential to synthesize an optimal controller that bridges the gap between control efficiency and operational flexibility.

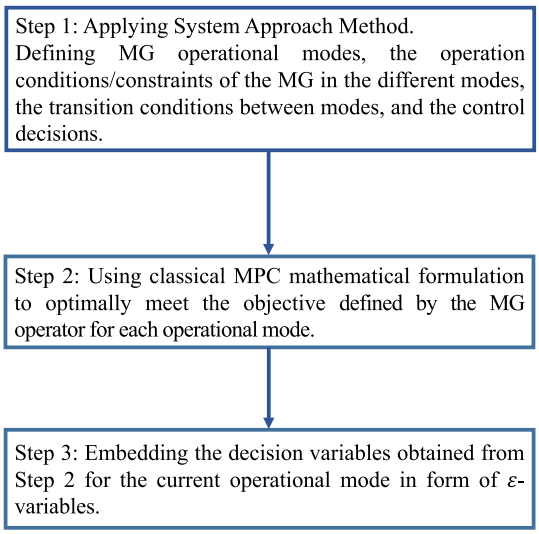

Fig. 1. Flow chart of the algorithm automatically generating S-MPC from the MPC.

This research is motivated by the need for a novel control methodology capable of providing optimal control for flexible MGs with PnP capabilities, addressing their specific operational modes and diverse energy resources. The primary contributions of this study include the synthesis of an innovative hybrid control method that incorporates the strengths of logic-based control and MPC. It allows for efficient control and supervision of MGs with the ability to seamlessly adapt to changing operational conditions while optimizing energy management.

This section presents the hybrid control method, outlining the various phases and procedures involved in the synthesis of the optimal controller. By combining the advantages of logic-based control and MPC and translating MPC decisions into ε-variables, this approach simplifies the complexity of controlling flexible MGs, making it easier to implement in practice. The subsequent sections detail the hybrid control method, its implementation, and simulation results that demonstrate its effectiveness in optimizing energy management in flexible MGs. This innovative approach offers a solution that aligns with the dynamic nature of MGs, enabling enhanced performance and increased integration of RESs.

3. Hybrid method to synthesize optimal controller for flexible MG with PnP capabilities

The methodology for building the controller of flexible hybrid MG comprises three key steps, as illustrated in Fig. 1. In the first step, the logical control system for the MG is built using a system approach method. In this step, the MG operational modes, the operation conditions/constraints of the MG in the different modes, the transition conditions between modes, and the control decisions are defined. The system approach used in this paper is the ε-variables presented in [28,29,32]. The controller obtained from the first step is a non-optimal controller. In the second step, the obtained controller will be used as input to generate the mathematical problem to optimally meet the objective defined for each operational mode, considering the operational condition already included in the controller obtained from Step 1. The controller resultant from Step 2 will be in the form of S-MPC. The S-MPC is then solved using the quadratic programming (QP) approach. During the solving stage in Step 2, the system inputs, states, and outputs are made in compact form. Finally, the controller formulated as S-MPC controls the MG in the different operational modes optimally. After finding the "optimal control decisions" in Step 2, these decisions will be

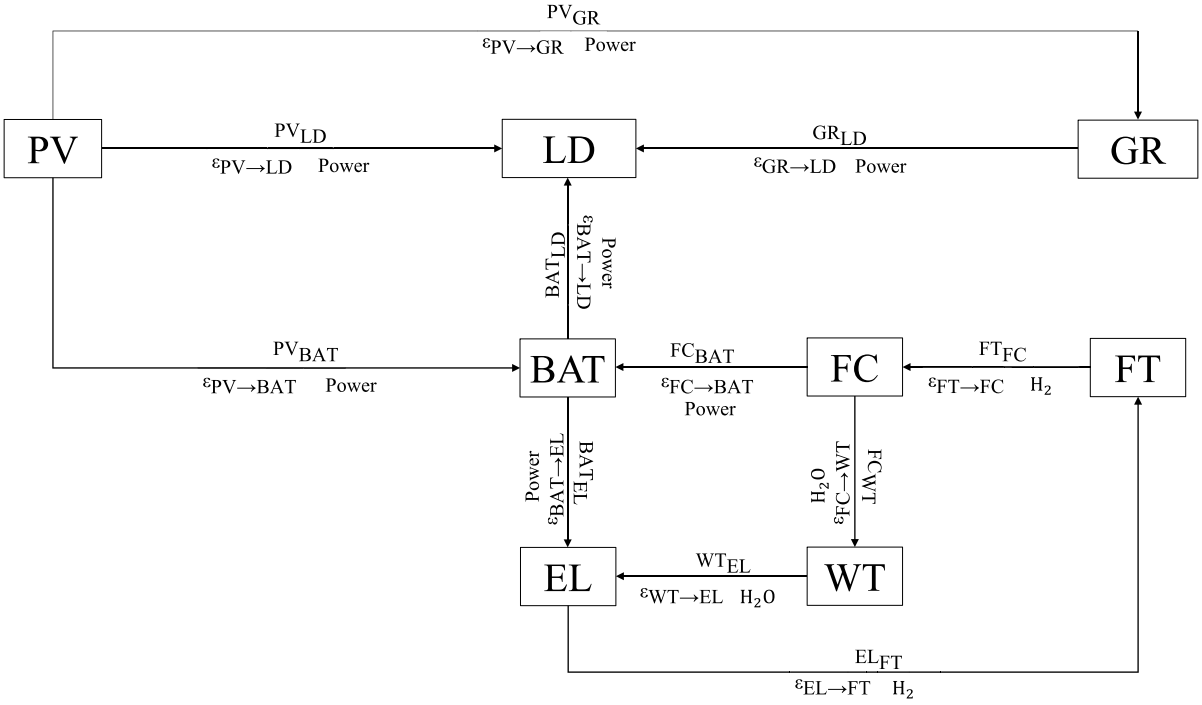

Fig. 2. Hybrid MG Structure.

embedded again in the form of ε-variables in Step 3. The output of Step 3 will be hence optimal ε-variables to control the MG. It is important to highlight the output of Step 1 is a controller in the form of non-optimal ε-variables.

During the operation of MG, the MG specifications, operator inputs, and the MG's assets will be checked at the beginning of each time step. If this information has been modified/changed or the MG structure has been modified, the operational mode of the MG will be updated accordingly, and the three steps of the controller building will be repeated to consider the modification. If not, the optimal ε-variables-based-controller already built will be used to control the MG for the next time step.

This comprehensive model serves as the basis for our proposed control strategy and energy management approach. It facilitates the quantification of interactions and relationships within the MG, enabling the derivation of an objective function that aligns with the system's goals and constraints. With this model in place, we can now proceed to the derivation and formulation of the objective function, which is central to optimizing the control decisions for the flexible MG. The model also allows us to define operational modes, system states, and optimize energy flows, providing a holistic view of the MG's functioning.

4. Detailed description of controller synthesizing method

The method suggested in this paper and outlined in Section 3 is a general method; however, in this section and for the sake of clarity, we will demonstrate the implementation of this method on a specific MG. Hence, this MG will be first introduced in this section. Then, each step shown in Fig. 1 and illustrated in Section 3 will be implemented.

One of the key contributions of our proposed method is the seamless integration of switching conditions into the operational model of the flexible MG. This integration allows for a more adaptive and responsive energy management strategy.

- **Defining Operational Modes**: In our model, the concept of operational modes is a fundamental building block. We define these operational modes to represent different states or conditions of the MG. Each operational mode is associated with a specific set of assets, energy flows, and operational constraints. This definition is achieved through the use of a system graph where nodes represent assets, and edges represent energy or matter flows, as described in Section 4.
- **Switching Conditions**: Switching conditions serve as the triggers that guide the transition between operational modes. These conditions are derived from the system graph and are formulated based on the logical control system approach. By identifying specific events or criteria within the MG, we determine when a transition from one operational mode to another is required.
- **Improving the Operation Strategy**: The integration of switching conditions into our operational model enhances our operation strategy in the following ways:
  - **Adaptability**: The MG can quickly adapt to changing circumstances by identifying when specific assets or power flows need to be engaged or disengaged based on the predefined switching conditions. For instance, when excess energy is generated by the PV arrays, the switching conditions can trigger the mode transition to store this surplus energy in the battery or other accumulators.
  - **Optimization**: The operation strategy aims to optimize energy flows and resource utilization. By linking switching conditions to operational modes, we can strategically direct energy and resources to where they are most needed at any given moment. This optimization helps in reducing reliance on the grid and improving the overall efficiency of the MG.

4.1. Microgrid description

This is a case study, and this is a real system that was built in Xanthi, Greece [32]. As shown in Fig. 2, the MG consists of a 15 kW PV array, a battery (BAT), a water tank (WT), and a fuel tank (FT) used as energy storage systems (ESSs), an electrolyzer (EL), a fuel cell (FC), the utility grid (GR). The PV can be used as a priority energy source on the MG. If the PV is not able to provide enough power, then either the BAT or the FC will ensure that the load is satisfied. The GR will supply the energy if the battery is empty and there is no available hydrogen. On the other

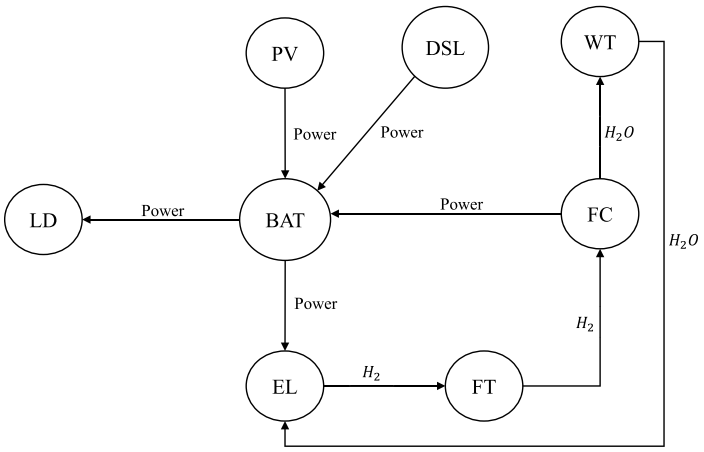

Fig. 3. Representing of hybrid energy system using graph method.

hand, when the BAT is full and there is a surplus, then the EL will be used if there is space in the WT and in the FT. Then, the energy will be sent to the GR.

The implementation of the methodology presented in Section 3 is summarized by the flowchart given in Fig. 1. In the following, each step of the implementation method will be explained for the MG shown in Fig. 2.

4.2. Step 1: Defining the operational modes and switching conditions (the logical control system approach)

A hybrid energy system can be defined as a set of power sources, including RES, as well as loads, storage equipment, and other devices that enable the transfer of energy and/or matter. The utilization of a directed graph to depict a MG is a widely recognized method, as evidenced by the work of [32]. This methodology has been demonstrated to significantly streamline the examination, investigation, formulation, and ultimately the optimal functioning of hybrid energy systems. In this context, each individual device is symbolized by a node, while the connection between the devices is denoted by an arrow, or an edge, which signifies the transfer of energy or matter between two nodes.

The main idea behind the ε-variable method is that every asset is symbolized by a node, and every flow of matter/energy is symbolized by an edge in the complicated MG system, as demonstrated in Fig. 3. Using this theory and the aforementioned evolution operators, this power system's analysis, management, and operation can be simplified. This method states that any hybrid power system consists of three key factors: converters, accumulators, and flows. The converters are used to convert the energy/matter to matter/energy, the accumulators accumulate energy/matter, and the flows symbolize the flow of energy/matter. Lastly, the control statements are the evolution operators based on the logical operators, illustrating the different types of EMSs exploited by the multi-vector system [32].

To implement our proposed method, the state graph is generated in **Point 1** as illustrated in Fig. 5. Then in **Point 2**, the different assets in each state will be classified as a converter, energy flow, or accumulator. The output of **Point 2** is the graph shown in Fig. 4. In **Point 3**, the dynamical state-space model is for each asset in each state. Using this theory and the evolution operators (calculated in Fig. 6), this power system's analysis, management, and operation can be simplified. This method states that any hybrid power system consists of three key factors: converters, accumulators, and flows. The converters are used to convert the energy/matter to matter/energy, the accumulators accumulate energy/matter, and the flows symbolize the flow of energy/matter. Lastly, the control statements are the evolution operators based on the logical operators, illustrating the different types of energy management systems (EMSs) exploited by the multi-vector system [27].

To control the flexible hybrid MG using logic control, state transition diagrams, also known as state machines or automata, can be used to represent the different operating modes of the accumulators. Different operational modes, switching conditions, and state variables in each mode are determined using binary notation. Each state in this diagram represents a particular mode or condition of the accumulators. The transitions between states represent the actions or events that cause the accumulators' mode to change. Fig. 4 depicts the various operating modes and relationships between them for a system comprised of a battery, a fuel tank, and a water tank via an automata graph. A three-digit binary number on the graph represents each of the eight possible states. The state "000" indicates that the system is completely off, whereas the state "111" indicates that all three components are charged or filled and the system is fully operational. The remaining six states represent various combinations of component charging or filling. Notably, the graph also displays the relationships between the various states. For instance, when the battery is charged and the water tank fills, the system can transition from state "000" to state "110." The system can transition from state "110" to state "010" if the battery is discharged while the water tank fills.

As evidence of the idea, Fig. 2 illustrates the hybrid MG system. According to the graph theory, the converters are the PV array, LD, GR, FC, and EL; the BAT, FT, and WT can be considered accumulators, and power, hydrogen, and water can be regarded as flows. As can be seen in Fig. 2, the assets of the MG system can be split into two sets as follows:

- The set of converters: $Rs^{Con} = \{PV,\ LD,\ GR,\ EL,\ FC\}$
- The set of accumulators: $Rs^{Acc} = \{BAT, FT, WT\}$

In addition, the connection between two nodes can be called a $flow$, such as FC to BAT and BAT to EL as a power flow, EL to FT and FT to FC as a hydrogen flow, and FC to WT and WT to EL as a hot water flow.

Therefore, the set of flows for the hybrid power system can be illustrated as follows [32]:

- The set of flows: $Flows = \{Power, Hydrogen, Water\}$

As shown in Fig. 4, to identify any dynamical system, we require two tasks (**Point 3**): (a) the set of its possible states (state space - S) and (b) an evolution operator (ϕ) that determines which specific state the system will be in at any given time. In this regard, the state s (**Point 4**) of a graph (i.e. of the MG) at a specific instant is given by the states of the nodes and edges specified as follows:

- A state (**Point 5**) must specify its presence and the type/amount of flow it includes for the edges. This is symbolized by variable $F^{j}_{a\to b}$ with $j \in Flow$ and $m,\ n$ two adjacent nodes. If there is no edge, $F^{j}_{a\to b}$ is zero.

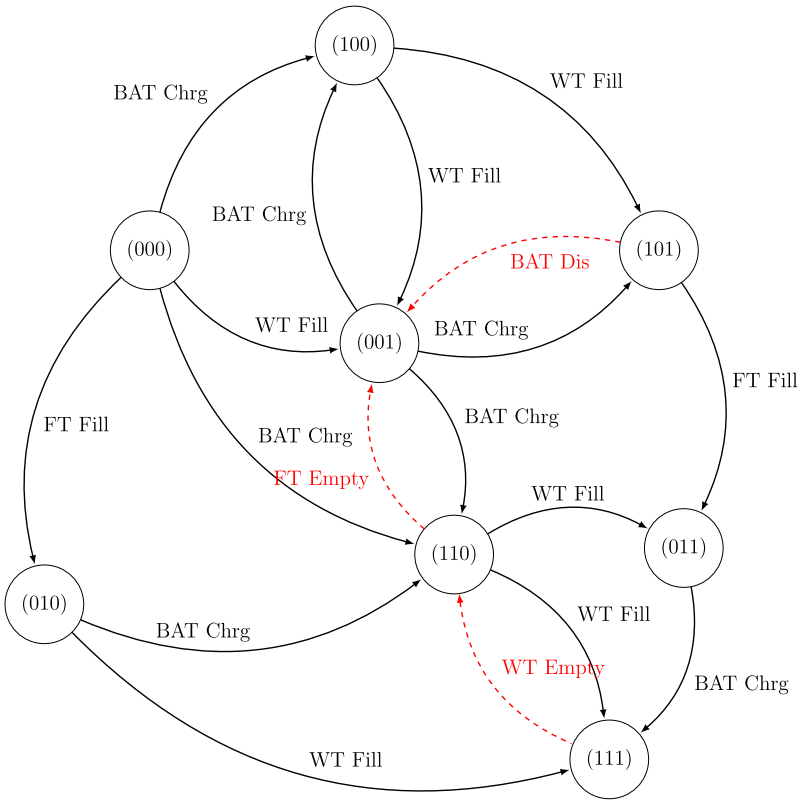

Fig. 4. The illustration of the different operational modes, the switching conditions, and the state variables in each mode using the automata/graph method.

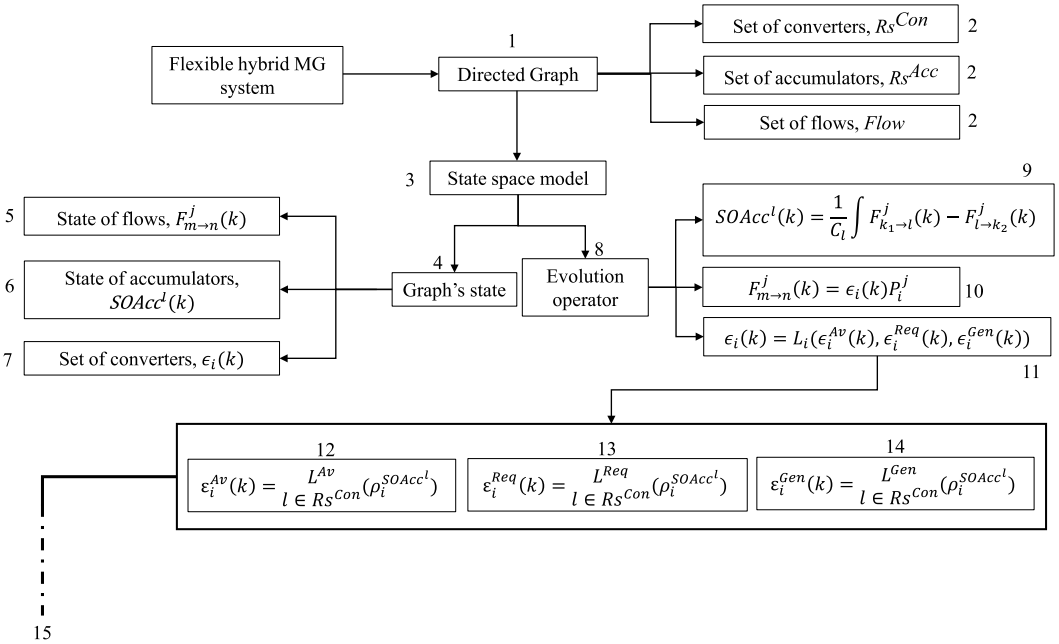

Fig. 5. A graph shown in state space (in the first step) for the hybrid control method; points addressed in the text are indicated by numbers.

- The state (**Point 6**) of an accumulator is the normalized amount of stored matter or energy, represented by variable $SOAcc^l \in [0,1]$, $l \in Rs^{Acc}$.
- The state (**Point 7**) of the converters is their status (whether they are activated or not), which is indicated by variable $\epsilon_i(k) \in 0,1$, $i \in Rs^{Con}$.

Hence, the states $s \in S$ of the graph are:

$$s = \{F^{j}_{a\to b}, SOAcc^{l}(k), \varepsilon_i(k)\}, \quad (1)$$

$$l \in Rs^{Acc},\ i \in Rs^{Con},\ a,b \in Rs^{Acc} x Rs^{Con},\ j \in Flow$$

The next step is to construct the evolution operator Φ (**Point 8**) so that given a state s in the state space S at an instant t_0; we can calculate the state at the instant t as $s(t) = \phi(t, s(t_0))$ where ϕ: $S \to S$.

This evolution operator is the energy management approach utilized to control the MG and the accumulator operation principle for our purposes. As in dynamical systems, we require a different evolution operator for each state variable, i.e., an evolution operator for each $s \in S$ in our graph.

The evolution operator (**Point 9**) for an accumulator l with a state variable $SOAcc^{l}$ is effectively an integrator and is dependent on its capacity C_l and the flows $F^{j}_{a\to b}(k)$ that are directed towards and away from the accumulator:

$$SOAcc^{l}(k) = SOAcc^{l}(k-1) + \frac{\sum_{k_1 \in Rs^{Con}}(F^{j}_{k_1\to l}(k)) - \sum_{k_2 \in Rs^{Con}}(F^{j}_{l\to k_2}(k))}{C_l} \quad (2)$$

An edge with the evolution operator $F^{j}_{a\to b}(k)$ (**Point 10**) has the following definition:

$$F^{j}_{a\to b}(k) = \varepsilon_i . P^{j}_{i},\ i \in \{m,n\},\ j \in Flow \quad (3)$$

where ε_i is the state of the corresponding converter and P^{j}_{i} is the amount of energy or matter that can be converted by the kth unit per unit of time. Variables P^{j}_{i} might be either uncontrollable (like the PV energy flow) or controlled by the grid's designer or the EMS (for example, the flow of energy from the FC).

Depending on the EMS, the evolution operator for the converters (i.e., the variables ε_i) (**Point 11**) can be a complex function. Nonetheless, it depends on three variables that have a binary representation:

1. $\varepsilon^{Av}_{i}(k)$, which stands for the availability of the material or energy to be transformed (**Point 12**).
2. A conversion's demand for materials or energy is represented by the symbol $\varepsilon^{Req}_{i}(k)$ (**Point 13**).
3. Other potential desired conditions (such as not operating the FC when the EVs are activated) that are not connected to the aforementioned are represented by $\varepsilon^{Gen}_{i}(k)$ (**Point 14**).

The state of the accumulators determines whether materials or energy are available or required to complete a conversion. A binary variable that is 1 when there is availability or demand and 0 otherwise is used to assess this:

$$\varepsilon^{Av}_{i}(k) = L^{Av}_{l\in Rs^{Acc}}(\rho^{SOAcc^{l}}_{i}) \quad (4)$$

$$\varepsilon^{Req}_{i}(k) = L^{Req}_{l\in Rs^{Acc}}(\rho^{SOAcc^{l}}_{i}) \quad (5)$$

where the logical operators L^{Av} and L^{Req} are used on the variables to quantify the need for and the supply of/from the accumulator l.

The general condition may be dependent on a node or an edge, but it is typically dependent on the state of other converters and can be characterized as follows:

$$\varepsilon^{Gen}_{i}(k) = L^{Gen}_{l\in Rs^{Con}}(\rho^{SOAcc^{l}}_{i}) \quad (6)$$

where L^{Gen} is a logical operator.

Using a logical operator L_i, the device i's final evolution operator is found:

$$\varepsilon_i(k) = L_i(\varepsilon^{Av}_{i}(k), \varepsilon^{Req}_{i}(k), \varepsilon^{Gen}_{i}(k)) \quad (7)$$

As shown in Fig. 6, this step is composed of sub-steps which are:

- Initially, evolution operators are defined.
- The power flows are calculated by multiplying equation P^{j}_{i} and Eq. (7). However, to calculate the EL and FC, some equations need to be as follows:
  According to Faraday's Law, the generation rate of H_2 in the EL and production rate of hot water in the FC can be calculated by respectively [15]:

$$n_{H_2} = n_F(n_c I_{elec})/(n_e F) \quad (8)$$

$$n_{H_2O} = (n_{c_{FC}} I_{FC})/(n_F)(n_e F) \quad (9)$$

  n_F symbolizes that Faraday's efficiency can be defined as the ratio between the actual and theoretical amount of H_2 generated and is generally between 80%–100%. I_{elec} and I_{FC} are the operating current for the EL and FC, respectively F is the Faraday's constant; n_c and $n_{c_{FC}}$ is the number of cells for the EL and FC, respectively; lastly, n_e is the number of electrons.

When the battery is fully charged, excess energy from the PV can potentially be exploited to run the electrolyzer at 4 kW. On the other hand, the PV does not accomplish to meet the load-generation mismatch; the fuel cell rated at 1 kW can be utilized in order to store hydrogen in the hydrogen tank. It can be used as an alternative energy. It can be used as an alternative energy. The generated water from the fuel cell is stored in the water tank. Optionally, the utility grid can be used in case of austere conditions, such as a lack of energy in the PV or accumulators. The power flows (in Fig. 2) of FC and EL can be calculated as follows:

- For the FC in Fig. 2;

$$F_{out\_}FC_{H_2O}(k) = \epsilon_{FC}(k) n_{H_2O} \quad (10)$$

$$F_{out\_}FC_{Power}(k) = \epsilon_{FC}(k) F_{FC} \quad (11)$$

$$F_{in\_}FT_{H_2}(k) = F_{out\_}EL_{H_2}(k) \quad (12)$$

  where $F_{out\_}FC_{H_2O}$ represents the flow of water from the FC to the water tank, $F_{out\_}FC_{Power}$ is the power from the FC to the battery, and $F_{in\_}FT_{H_2}$ is the flow of hydrogen from the FT to the FC. ε_{FC} can be defined as the final evolution operator of the fuel cell.
- For the EL in Fig. 2;

$$F_{in\_}BAT_{Power}(k) = F_{out\_}PV_{Power}(k) + F_{out\_}GR_{Power}(k) + F_{out\_}FC_{Power}(k) \quad (13)$$

$$F_{in\_}WT_{H_2O}(k) = F_{out\_}FC_{H_2O}(k) \quad (14)$$

$$F_{out\_}EL_{H_2}(k) = \epsilon_{EL}(k) n_{H_2} \quad (15)$$

  where $F_{in\_}BAT_{Power}$ is the total power in the BAT. $F_{out\_}PV_{Power}$ is the power for the load, battery, and utility grid. $F_{out\_}GR_{Power}$ is the power for the load. $F_{in\_}WT_{H_2O}$ is the water from the FC. $F_{out\_}EL_{H_2}$ is the flow from the EL to the FT.
  Also, consider these equations:

$$F_{out\_}FT_{H_2}(k) = \epsilon_{FC}(k) n_{H_2O} \quad (16)$$

$$F_{out\_}BAT_{Power}(k) = \epsilon_{EL}(k) F_{EL} \quad (17)$$

$$F_{out\_}WT_{H_2O}(k) = \epsilon_{EL}(k) n_{H_2} \quad (18)$$

$$F_{out\_}PV_{Power}(k) = \epsilon_{PV}(k) F_{out\_}PV(k) \quad (19)$$

$$F_{out\_}GR_{Power}(k) = \epsilon_{GR}(k) F_{out\_}GR(k) \quad (20)$$

  where $F_{out\_}FT_{H_2}$ represents the flow of hydrogen from FT to the EL, $F_{out\_}BAT_{Power}$ is the power from the BAT to the EL, $F_{out\_}WT_{H_2O}$ is the flow of water from the WT to the EL.
- The last step is to calculate the evolution operator for the accumulators (see Eq. (2)).

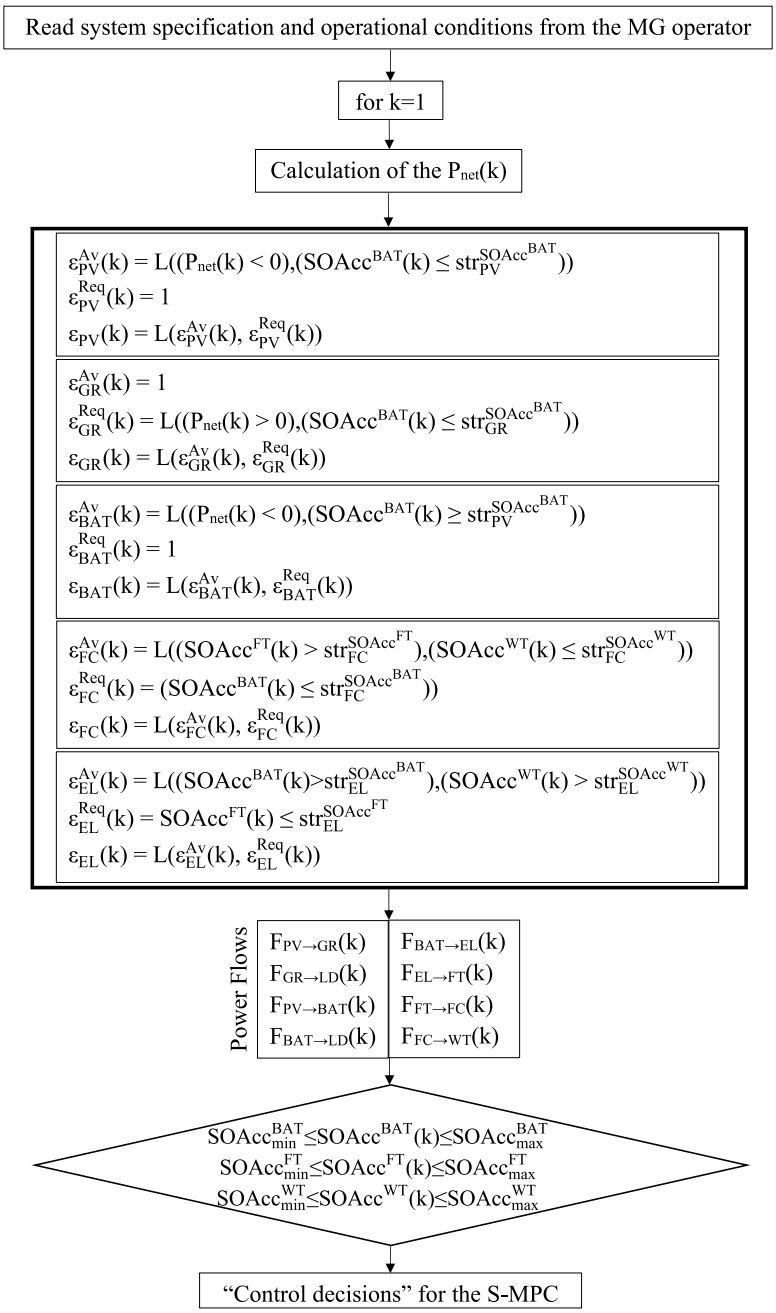

Fig. 6. The flow chart of the ε-variables.

4.3. Step 2: Generating the optimal controller for each operational mode

From Step 1, the control decisions obtained are utilized to find the optimum system control, state, and output vectors for the S-MPC. There are several stages as follows (**Point 15**):

Define the system-state, control, and output vectors for the MG with the help of Eq. (2)–(3) and (7). From Eq. (7), the system-state vector of the MG is defined as follows (**Point 15**) (see Fig. 7):

$$x_{a_1}(k) = [SOAcc^{BAT}(k)] \tag{21}$$

$$x_{a_2}(k) = [SOAcc^{FT}(k)] \tag{22}$$

$$x_{a_3}(k) = [SOAcc^{WT}(k)] \tag{23}$$

$SOAcc^{BAT}(k)$, $SOAcc^{FT}(k)$, and $SOAcc^{WT}(k)$ are the state of accumulators for the battery, hydrogen tank, and water tank, respectively. x_{a_1}, x_{a_2}, and x_{a_3} can be defined as parts of the sub-state vector of the MG system. From Eqs. (3) and (10)–(20), the system-control (input) vector of the MG is found as follows (**Point 15**):

$$\begin{aligned} u(k) = [&PV_{LD}(k); GR_{LD}(k); PV_{BAT}(k); \\ &BAT_{LD}(k); FC_{BAT}(k); BAT_{EL}(k); \\ &EL_{FT}(k); FT_{FC}(k); WT_{EL}(k)] \end{aligned} \tag{24}$$

The dynamic process equations of the battery, hydrogen, and water tank can be represented by:

$$\begin{aligned} x_{a_1}(k) &= x_{a_1}(k-1) + b_{a_1}u(k-1) \\ \Delta x_{a_1}(k) &= b_{a_1}u(k-1) \end{aligned} \tag{25}$$

where $b_{a_1} = [0 \;\; 0 \;\; \eta_{ch} \;\; -\eta_{dis} \;\; \eta_{ch} \;\; -\eta_{dis} \;\; 0 \;\; 0 \;\; 0 \;\; 0]$.

$$\begin{aligned} x_{a_2}(k) &= x_{a_2}(k-1) + b_{a_2}u(k-1) \\ \Delta x_{a_2}(k) &= b_{a_2}u(k-1) \end{aligned} \tag{26}$$

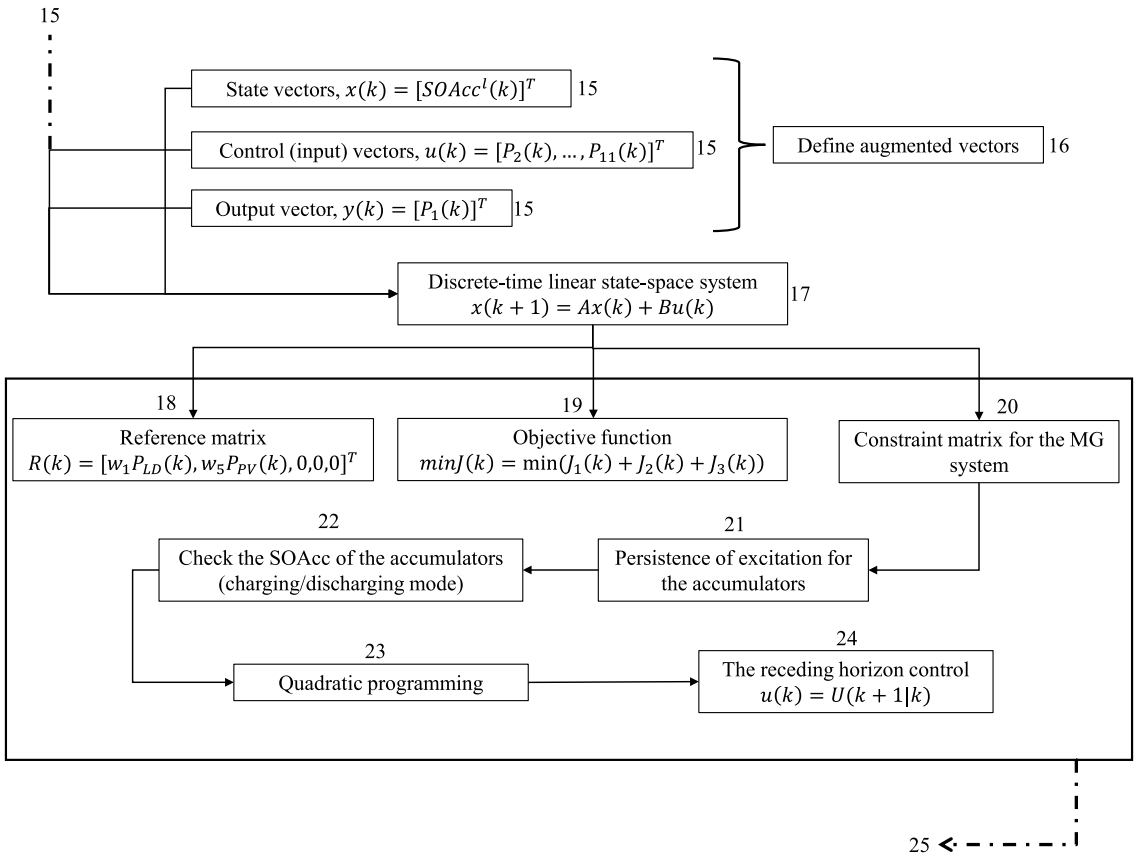

Fig. 7. A graph is shown in the second step for the hybrid control method; points addressed in the text are indicated by numbers.

where $b_{a_2} = [0\ 0\ 0\ 0\ 0\ 0\ \eta_{ch_{H_2}}\ -\eta_{dis_{H_2}}\ 0\ 0]$.

$$x_{a_3}(k) = x_{a_3}(k-1) + b_{a_3}u(k-1)$$
$$\Delta x_{a_3}(k) = b_{a_3}u(k-1) \tag{27}$$

where $b_{a_3} = [0\ 0\ 0\ 0\ 0\ 0\ 0\ 0\ \eta_{ch_{H_2O}}\ -\eta_{dis_{H_2O}}]$.

The system-output vector of the MG is as follows (**Point 15**):

$$y_a(k) = c_a x_a(k-1) + d_a u(k) \tag{28}$$

where $c_a = 0$ and $d_a = [w_1\ \ w_1\ \ 0\ \ w_1\ \ 0\ \ 0\ \ 0\ \ 0\ \ 0\ \ 0]$. From the definition of y_a,

$$\sum (w_1 P_{LD}(k) - y_a(k))^2 \tag{29}$$

where w_1 is a positive weight coefficient for the minimization of the operational cost of the hybrid MG. where w_i is the weighting coefficient and satisfying $w_i \in (0,1)$ and $i \in \{1,2,3,4,5\}$. The solutions of the multi-objective problem will exhibit a high degree of sensitivity to variations in the weighting coefficient [33].

$$y_b(k) = w_3(P_2(k) + P_4(k)) = c_b x_a(k-1) + d_b u(k) \tag{30}$$

With respect to y_b, where w_1 is a positive weight coefficient for the minimization of the operational cost of the hybrid MG. P_2 and P_4 are the power flows representing the PV to the load, PV_{LD} and PV to the battery, PV_{BAT}, respectively.

where $c_b = 0$ and $d_b = [w_3\ \ 0\ \ w_3\ \ 0\ 0\ 0\ 0\ 0\ 0\ 0]$. To increase the exported energy, the definition of y_b,

$$\sum (w_5 P_{PV}(k) - y_b(k))^2 \tag{31}$$

where w_3 is a positive weight coefficient for the enhancement of usage of the PV generator. Regarding y_c, y_d, and y_e,

$$\begin{aligned} y_c(k) &= w_2(P_4(k) + P_5(k) + P_6(k) + P_7(k)) \\ &= c_c x_a(k-1) + d_c u(k) \end{aligned} \tag{32}$$

where $c_c = 0$ and $d_c = [0\ \ 0\ \ w_2\ \ w_2\ \ w_2\ \ w_2\ \ 0\ \ 0\ \ 0\ \ 0]$. P_5, P_6, and P_7 are the power flows representing the battery to the load, BAT_{LD}, the fuel cell to the battery, FC_{BAT}, and the battery to the electrolyzer, BAT_{EL}, respectively. To penalize the accumulators, the definition of y_c,

$$\sum y_c(k)^2 + y_d(k)^2 + y_e(k)^2 \tag{33}$$

where w_2 is a positive weight coefficient for the penalization of the battery utilization. y_d and y_e (for other accumulators) can be found in a similar way.

Define the augmented system-states (**Point 16**):

$$\begin{aligned} x(k) = [&x_{a_1}(k); x_{a_2}(k); x_{a_3}(k); y_a(k-1); \\ &y_b(k-1); y_c(k-1); y_d(k-1); y_e(k-1)] \end{aligned} \tag{34}$$

Define the augmented system output (**Point 16**):

$$\begin{aligned} y(k) = [&y_a(k-1); y_b(k-1); y_c(k-1); \\ &y_d(k-1); y_e(k-1)] \end{aligned} \tag{35}$$

where y_a, y_b, y_c, y_d, and y_e can be defined as parts of sub-output vector of the MG system. Consider the discrete-time linear state-space system (**Point 17**) [34]:

$$x(k+1) = Ax(k) + Bu(k) \tag{36}$$

where $k = 0, 1, 2, \ldots, N_p - 1$ symbolizes the discrete-time instant; $x(k)$ is the system-state vector; $u(k)$ and $y(k)$ are the system-control vector and system-output vector, respectively. N_p is the number of future control intervals called the prediction horizon.

The linear state-space equation can be stated depending on the battery, fuel tank, and water tank equations (see Eq. (2)).

Because of the dynamic equation of $SOAcc^{BAT}$, $SOAcc^{FT}$, and $SOAcc^{WT}$, in Eq. (2), the components A and B will be:

$$A = \begin{bmatrix} 1\ zeros(1,7);\ 0\ 1\ zeros(1,6);\ 0\ 0\ 1\ zeros(1,5); \\ zeros(5,8) \end{bmatrix}$$

$$B = \begin{bmatrix} 0 & 0 & \eta_{ch} & -\eta_{dis} & \eta_{ch} & -\eta_{dis} & 0 & 0 & 0 & 0 \\ 0 & 0 & 0 & 0 & 0 & 0 & \eta_{ch,\mathrm{H_2}} & -\eta_{dis,\mathrm{H_2}} & 0 & 0 \\ 0 & 0 & 0 & 0 & 0 & 0 & 0 & 0 & \eta_{ch,\mathrm{H_2O}} & -\eta_{dis,\mathrm{H_2O}} \\ w_1 & w_1 & 0 & w_1 & 0 & 0 & 0 & 0 & 0 & 0 \\ w_5 & 0 & w_5 & 0 & 0 & 0 & 0 & 0 & 0 & 0 \\ 0 & 0 & w_2 & w_2 & w_2 & w_2 & 0 & 0 & 0 & 0 \\ 0 & 0 & 0 & 0 & 0 & 0 & w_3 & w_3 & 0 & 0 \\ 0 & 0 & 0 & 0 & 0 & 0 & 0 & 0 & w_4 & w_4 \end{bmatrix}$$

Define the reference matrix (R) for the MG (**Point 18**):

$$R(k) = [w_1(P_{LD}(k); w_5(P_{PV}(k); 0; 0; 0; w_1(P_{LD}(k+1); w_5(P_{PV}(k+1); 0; 0; 0; \\ ; \ldots; w_1(P_{LD}(k+N_p-1); w_5(P_{PV}(k+N_p-1); 0; 0; 0] \tag{37}$$

Define the objective functions for the S-MPC on the MG (**Point 19**):

a. The utilization of the utility grid is minimized.

$$min\ J_1(k) = min \sum_{k}^{k+N_p} (w_1 P_{LD}(k) - y_a(k))^2 \tag{38}$$

b. The usage of the accumulators is penalized so as to prevent the charging from the utility grid

$$min\ J_2(k) = min \sum_{k}^{k+N_p} y_c(k)^2 + y_d(k)^2 + y_e(k)^2 \tag{39}$$

c. The exported energy to the utility grid is encouraged.

$$min\ J_3(k) = min \sum_{k}^{k+N_p} (w_3 P_{PV}(k) - y_b(k))^2 \tag{40}$$

Define the overall cost function (objective function) for the MG:

$$min\ J(k) = min\ (J_1(k) + J_2(k) + J_3(k)) = (Y(k) - R(k))^T (Y(k) - R(k)) \tag{41}$$

where $(Y(k) = ((y(k+1|k), y(k+2|k), y(k+3|k), \ldots, y(k+N_P|k)))^T)$

Define the constraints for the MG as follows (**Point 20**):

Energy/matter flows from the PV array, utility grid, battery, fuel tank, electrolyzer, fuel cell, and water tank are non-negative values and are subject to their maximum values.

$$\begin{aligned} 0 \le P_1(k) = P_{LD}(k) - y_a(k) \le P_1^{max} \\ 0 \le P_m(k) \le P_m^{max} \end{aligned} \tag{42}$$

where P_m^{max} $(m = 1, 2, \ldots, 11)$ imply the maximum values of energy/matter flows. The sum of PV energy supplied directly for the load $(P_2(k))$ and the battery for the charging $(P_4(k))$ should be smaller than the energy flow from the PV array, $(P_{PV}(k))$.

$$P_2(k) + P_4(k) \le P_{PV}(k) \tag{43}$$

The $SOAcc^{BAT}$ for the battery, $SOAcc^{FT}$ for the fuel tank, and $SOAcc^{WT}$ for the water tank are restricted between their minimum and maximum values [29].

$$\begin{aligned} SOAcc^{BAT^{min}} \le SOAcc^{BAT} \le SOAcc^{BAT^{max}} \\ SOAcc^{FT^{min}} \le SOAcc^{FT} \le SOAcc^{FT^{max}} \\ SOAcc^{WT^{min}} \le SOAcc^{WT} \le SOAcc^{BAT^{WT}} \end{aligned} \tag{44}$$

Charging and discharging for the battery, fuel tank, and water tank cannot happen simultaneously, as is implied by the following:

$$\begin{aligned} P_4(k)P_5(k) \le 0 \quad P_6(k)P_7(k) \le 0 \\ P_8(k)P_9(k) \le 0 \quad P_{10}(k)P_{11}(k) \le 0 \end{aligned} \tag{45}$$

It is worth noting that Eq. (42) and (43) are convex, whereas Eq. (45) is non-convex. In order to accomplish convex optimization in S-MPC design, the non-convex constraints into two switched cases: (i) charging: ($P_5 = 0, P_7 = 0, P_9 = 0$, and $P_{11} = 0$) and (ii) discharging: ($P_4 = 0, P_6 = 0, P_8 = 0$, and $P_{10} = 0$) (**Point 21**).

1. Charging: The constraint can be re-written by:

$$\begin{aligned} P_5(k) \le 0 \quad P_5(k) \ge 0 \\ P_7(k) \le 0 \quad P_7(k) \ge 0 \\ P_9(k) \le 0 \quad P_9(k) \ge 0 \\ P_{11}(k) \le 0 \quad P_{11}(k) \ge 0 \end{aligned} \tag{46}$$

Constraints (42), (43), and (46) can be compactly re-written by:

$$\mu_{ch} u(k) \le \gamma_{ch} \tag{47}$$

where

$$\mu_{ch} = \begin{bmatrix} & & & -eye(10) & & & & & & \\ 0 & 0 & 0 & 1 & 0 & 1 & 0 & 1 & 0 & 1 \\ 1 & 1 & 0 & 1 & 0 & 0 & 0 & 0 & 0 & 0 \\ 1 & 0 & 1 & 0 & 0 & 0 & 0 & 0 & 0 & 0 \\ & & & eye(10) & & & & & & \\ -1 & -1 & 0 & -1 & 0 & 0 & 0 & 0 & 0 & 0 \end{bmatrix} \quad \gamma_{ch} = \begin{bmatrix} zeros(10,1) \\ 0 \\ P_{LD}(k) \\ P_{PV}(k) \\ P_m^{max} ones(10,1) \\ P_3^{max} - P_{LD}(k) \end{bmatrix}$$

where eye is an identity matrix, and $zeros$ is creating an array of all zeros.

2. Discharging: The constraint can be re-written by:

$$\begin{aligned} P_4(k) \le 0 \quad P_4(k) \ge 0 \\ P_6(k) \le 0 \quad P_6(k) \ge 0 \\ P_8(k) \le 0 \quad P_8(k) \ge 0 \\ P_{10}(k) \le 0 \quad P_{10}(k) \ge 0 \end{aligned} \tag{48}$$

Constraints (42), (43), and (48) can be compactly re-written by:

$$\mu_{dis} u(k) \le \gamma_{dis} \tag{49}$$

where

$$\mu_{dis} = \begin{bmatrix} & & & -eye(10) & & & & & & \\ 0 & 0 & 1 & 0 & 1 & 0 & 1 & 0 & 1 & 0 \\ 1 & 1 & 0 & 1 & 0 & 0 & 0 & 0 & 0 & 0 \\ 1 & 0 & 1 & 0 & 0 & 0 & 0 & 0 & 0 & 0 \\ & & & eye(10) & & & & & & \\ -1 & -1 & 0 & -1 & 0 & 0 & 0 & 0 & 0 & 0 \end{bmatrix} \quad \gamma_{dis} = \begin{bmatrix} zeros(10,1) \\ 0 \\ P_{LD}(k) \\ P_{PV}(k) \\ P_m^{max} ones(10,1) \\ P_3^{max} - P_{LD}(k) \end{bmatrix}$$

Define the predictive control vector for the MG:

$$U(k) = [u^T(k), u^T(k+1|k), \ldots, u^T(k+N_c|k)]^T \tag{50}$$

where $u(k+m|k)$ is the predicted value of u from the sampling time k and N_c is the number of control (input) moves to be optimized at sampling time k called the control horizon. Because each $u(k+m|k)$ in the predictive control vector $U(k)$ should satisfy (35) and (37), it follows that $U(k)$ should satisfy:

$$\overline{\mu}_{ch} U(k) = \overline{\gamma}_{ch} \tag{51}$$

where

$$\overline{\mu}_{ch} = \underbrace{\begin{bmatrix} \mu_{ch} & \cdots & 0 \\ \vdots & \ddots & \vdots \\ 0 & \cdots & \mu_{ch} \end{bmatrix}}_{N_c} \quad \overline{\gamma}_{ch} = \begin{bmatrix} \gamma_{ch} \\ \vdots \\ \gamma ch \end{bmatrix}$$

$$\overline{\mu}_{dis} U(k) = \overline{\gamma}_{dis} \tag{52}$$

where

$$\overline{\mu}_{dis} = \underbrace{\begin{bmatrix} \mu_{dis} & \cdots & 0 \\ \vdots & \ddots & \vdots \\ 0 & \cdots & \mu_{dis} \end{bmatrix}}_{N_c} \quad \overline{\gamma}_{dis} = \begin{bmatrix} \gamma_{dis} \\ \vdots \\ \gamma dis \end{bmatrix}$$

Design and control the multiple models depending on several parameters as follows (**Point 22**):

if $\varepsilon_i P_i^j < 0; \quad SOAcc^l > SOAcc^{l^{min}}$

$$SOAcc^{l} < SOAcc^{l^{max}}$$

$$\text{if} \quad \epsilon_i P_i^j > 0; \quad SOAcc^{l} > SOAcc^{l^{max}}$$

$$SOAcc^{l} < SOAcc^{l^{min}}$$

Then, minimize the quadratic cost function as follows (**Point 23**):

$$J(U) = \sum_{k=0}^{N_p-1} (x(k)^T Q x(k) + u(k)^T C x(k)) + x(N)^T Q_f x(k) \tag{53}$$

where N is called the horizon of the quadratic problem. Q is the state weight $Q = Q^T \geq 0$; C is the control weight $C = C^T > 0$ and Q_f is the final cost weight $Q = {Q_f}^T \geq 0$.

Note that $X = (x(0), x(1), \ldots, x(N))$ is a linear function of $x(0)$ and $U = (u(0), u(1), \ldots, u(N-1))$.

$$\begin{bmatrix} x(0) \\ x(1) \\ \vdots \\ x(N) \end{bmatrix} = \begin{bmatrix} 0 & 0 & \cdots & 0 \\ B & 0 & \cdots & 0 \\ AB & B & 0 & \vdots \\ \vdots & \vdots & \ddots & 0 \\ A^{N-1}B & A^{N-2}B & \cdots & B \end{bmatrix} \begin{bmatrix} u(0) \\ u(1) \\ \vdots \\ u(N-1) \end{bmatrix} + \begin{bmatrix} I \\ A \\ A^2 \\ A^N \end{bmatrix}$$

This matrix can be expressed as:

$$X = GU + Hx(0) \tag{54}$$

where $G \in \mathbb{R}^{Nn.Nm}$ and $H \in \mathbb{R}^{Nn.Nn}$.

Eq. (53) can be re-written as follows:

$$J(U) = X^T \underbrace{\begin{bmatrix} Q & 0 & \cdots & 0 \\ 0 & \ddots & 0 & \vdots \\ \vdots & 0 & Q & 0 \\ 0 & \cdots & 0 & Q_f \end{bmatrix}}_{Q_1} X + U^T \underbrace{\begin{bmatrix} R & 0 & \cdots & 0 \\ 0 & \ddots & 0 & \vdots \\ \vdots & 0 & R & 0 \\ 0 & \cdots & 0 & R_f \end{bmatrix}}_{Q_2} U$$

These matrices are combined with Eq. (54) to obtain Eq. (55) using the QP:

$$J(U) = (GU + Hx(0))^T Q_1 (GU + Hx(0)) + U^T Q_2 U \tag{55}$$

The calculation of receding horizon control (**Point 24**):

In the S-MPC principle, the optimization problem is solved during each sampling time k, and the first element of $U(k)$ is employed to the MG:

$$u(k) = U(k+1|k) \tag{56}$$

4.4. Step 3: Implementing the optimal decisions using the logical control system approach

As illustrated in Fig. 13, in this section, the utility grid (PV_{GR} and GR_{LD}) is removed (the MG is working in islanded mode), and the EV fleet that their batteries have 45 kWh, 55 kWh, and 60 kWh (EV_{LD}) are added, and the state space is updated (**Point 25**). Then, the power flows are re-calculated by multiplying Eq. (7) and (24) (**Point 26**) (see Fig. 8).

$$F^j_{a\to b}(k) = u(m)\epsilon_i(k) \tag{57}$$

$$F^{Power}_{EV\to LD}(k) = P_{net}(k)\epsilon_i(k) \tag{58}$$

$$F^{Power}_{PV\to EV}(k) = P_{net}(k)\epsilon_i(k) \tag{59}$$

where $u(m)$ is the control variables of the S-MPC for m=2,4, …,11. After that, another step is to measure the evolution operator for the accumulators (BAT, FT, and WT) (see Eq. (2)) (**Point 27**).

Finally, the hybrid control method is checked to determine whether the system specifications/inputs of the flexible hybrid MG operator changed for the next time step or not (removing the utility grid and adding the EV fleet).

If YES, the operational assets of the flexible hybrid MG are updated (**Point 28**), and the system goes back to the first step to implement the standard ϵ-variables (**Point 29**). Then, all three steps are re-implemented.

If NO, the next step is to go back to the "optimal control decisions" (**Point 30**). Then, the third step (optimal ϵ-variables) is re-implemented.

In summary, to simply the hybrid control method is composed of several phases:

- Some system specifications and operational conditions from the flexible hybrid MG operator, such as PV and load data, and some parameters, including battery, fuel tank, and water tank, are defined.
- Net energy P_{net} (differences between the PV and the load data for 48 h and 8760 h) is calculated. However, net energy for the FC and EL is calculated according to Eq. (8)–(20)
- The evolution operators for the accumulators and converters are calculated; then, the power flows among the components of the hybrid MG are calculated.
- The last step in the ϵ-variables is the measurement of the $SOAcc$ for the BAT, FT, and WT.
- The first step in the S-MPC is to evaluate the "control decisions" obtained by exploiting the standard (non-optimal) ϵ-variables.
- The A, B, u, x, and y matrices are obtained depending on the "control decisions".
- Multiple models are evaluated for the accumulators, depending on the amount of power P_i^j and $SOAcc^l$.
- After that, the persistence of excitation for the accumulators (BAT, FT, and WT) is implemented in order not to allow the charging and discharging conditions for the accumulators simultaneously.
- The hybrid MG system is optimized with the help of "quadratic programming".
- The state of the accumulators for the battery, fuel tank, and water tank is updated.
- "Optimal control decisions" are measured and compared with former "control decisions".
- In the final step, these "optimal control decisions" are embedded in the ϵ-variables-based EMS.
- The $SOAcc$ for the BAT, FT, and WT is measured and updated. The output of the last step will be thus optimal ϵ-variables-based EMS.
- The MG requirements and inputs from the MG operator will be checked at the start of each time step during the operating phase of the EMS. If this information is adjusted or changed, the operating states of the MG assets are updated, and the three steps of EMS construction are performed to take the new input into account. If this is not the case, the best ϵ-variables-based EMS can be utilized to regulate the MG for the following time step. It is worth noting that the suggested method determines whether or not the MG operator's system specifications/inputs change for the next time step.

5. Simulation results and discussions

In this section, the simulation results of four use cases are presented. In the first two use cases, the MG is controlled using logical control, and S-MPC is built using the method explained in Sections 3 and 4. The aim of these two use cases is to show the optimality of the built controller. The capability of the controller to deal with PnP assets is demonstrated in use case 3. Finally, the flexibility of the controller to manage optimal energy flow when the MG moved from one operational mode to another operational mode is demonstrated in use case 4. In case 4, the MG moves from grid-connected operational mode to islanded operational mode. Table 1 summarizes the several parameters

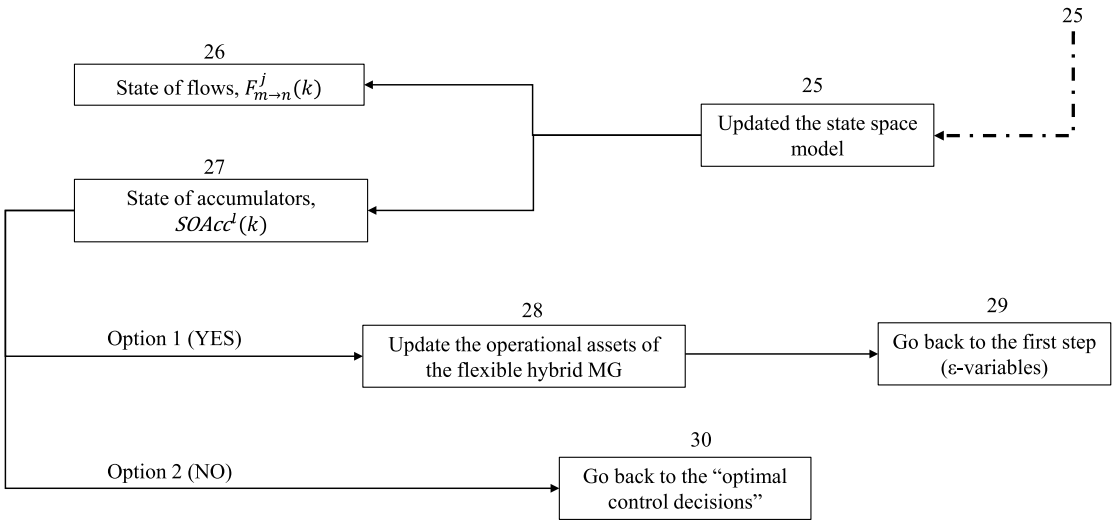

Fig. 8. A graph shown in the third step for the hybrid control method; points addressed in the text are indicated by numbers.

Table 1
Parameters for the real system [37].

Parameters for the real system		
$w_1 = 1.0$	$SOAcc^{BAT}(1) = 30\%$	$P^{max}_{m} = 5$ kW
$w_2 = 0.4$	$SOAcc^{FT}(1) = 90\%$	$C^{max}_{BAT} = 96$ kWh
$w_3 = 0.3$	$SOAcc^{WT}(1) = 50\%$	$C^{max}_{FT} = 10.1$ kWh
$w_4 = 0.5$	$F_{EL} = 4$ kW	$C^{max}_{WT} = 39.7$ kWh
$w_5 = 0.9$	$F_{FC} = 1$ kW	$SOAcc^{l}_{max} = 90\%$
$nc_{EL} = 15$	$nc_{FC} = 40$	$SOAcc^{l}_{min} = 20\%$
$\eta^{l}_{ch} = 0.9$	$\eta^{l}_{dis} = 0.85$	$\Delta t = 1$ h
$C^{max}_{EV_1} = 45$ kWh	$C^{max}_{EV_2} = 55$ kWh	$C^{max}_{EV_3} = 60$ kWh

used for our simulations which were also used in [35]. The data of the energy generation from the PV system and energy demand were obtained from [36], and our work is based on a real system as validated in [37].

In our proposed methodology, the control system is fundamentally a closed-loop control system, a type of control system that continuously monitors the current state of the system and makes real-time adjustments to control inputs based on feedback and system behavior. This type of control system is well-suited for dynamic and complex systems, such as flexible MGs, as it allows for adaptation to changing conditions and disturbances.

It is important to clarify that while MPC involves predictive modeling of the system's future behavior, it primarily falls under the category of closed-loop control. This is because MPC considers the current state of the system and adjusts control actions in real-time based on feedback and predicted future states to meet performance objectives. Our proposed methodology leverages MPC techniques within a closed-loop control framework to optimize control actions in flexible MGs with PnP capabilities. This closed-loop system is capable of adapting to various operational modes and changes in the MG's configuration, which is a crucial feature for effectively managing such complex systems.

5.1. Use case 1: Control of the flexible hybrid MG using logic control

The system's behavior is analyzed during the simulation of the flexible hybrid MG with logic control. Initially, the battery is in a discharging mode, as indicated by the digit 0 in the first position of the three-digit code, as shown in Fig. 9. As the simulation progressed, the PV system's output was utilized to satisfy the mismatch load demand. If the PV system generates excess energy, it is used to charge the battery, which occurred at the 13th time step. Consequently, the three-digit code is changed to (100) to indicate that the battery is in charging mode. At the 15th time step, the battery continued to charge, and the WT reached its maximum output. In this instance, the three-digit code is changed to (101) to indicate that the battery was in charging mode while the WT was being filled. After one hour, the battery is neither charging nor discharging, but the WT still is filling, so the three-digit code was updated to (001). Between the 16th and 22nd time steps, the battery is discharged. At the beginning of the 22nd and 30th-time steps, the FT is filling, and the utility grid is also used to compensate for the imbalance between load and generation. Throughout this time frame, the three-digit code was changed to (010). The three-digit code is updated to (110) after the PV system supplies power to the battery for one hour. The WT is fully filled at the 32nd time step, but the battery remains in charging mode. The three-digit code is therefore changed to (100). At the start of the 36th time step, the WT reached its maximum capacity, and the battery continued to charge, resulting in the update of the three-digit code to (101). The battery is neither charged nor discharged after three hours, while the WT remains at its maximum capacity. As a result, the three-digit code for these states was changed to (001).

The logic control approach in the control of the flexible hybrid microgrid exhibited distinct behavior, as indicated by the changing three-digit code, which reflected the operational modes of the accumulators and converters' utilization to manage load-generation imbalances. The analysis of these code variations provides valuable insights into the effectiveness of the control strategy in managing energy flow.

5.2. Use case 2: Controlling the flexible hybrid MG using S-MPC

The results of the standard ε-variables are utilized to obtain the components of the S-MPC, such as coefficient A and B, control (input) vector u, state vector x, and output vector y. At the end of the second step of the proposed method, the optimal control decisions are obtained. The increase in the exported energy and the decrease in the imported energy are the main significant advantages of S-MPC over MPC. To prove that, the controller has been simulated for one year (8760 h). Our results illustrate that the exported energy to the utility grid PV_{GR} is encouraged from 1705.35 kWh to 2571.01 kWh. Energy imported from the grid significantly decreased from 1494.36 kWh to 796.46 kWh, as demonstrated in Fig. 10. These results are expected and desired since the optimal control decisions are obtained using the S-MPC.

Quantitatively, the decrease in grid-supplied energy imports is approximately 46.9%, indicating a significant reduction in reliance

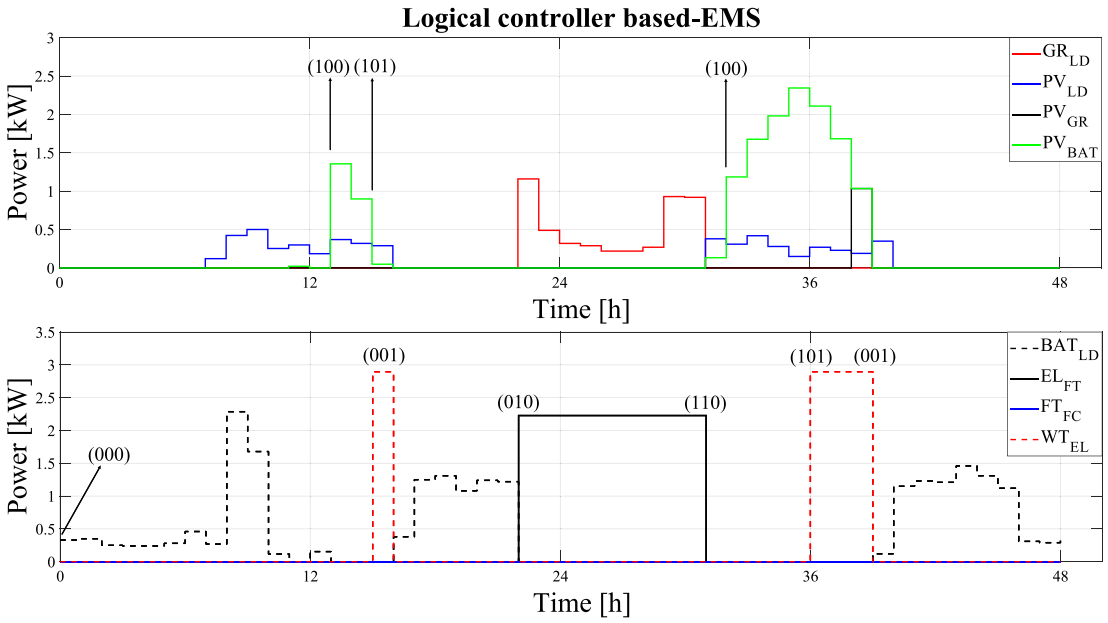

Fig. 9. The results of working of logical controller based-EMS.

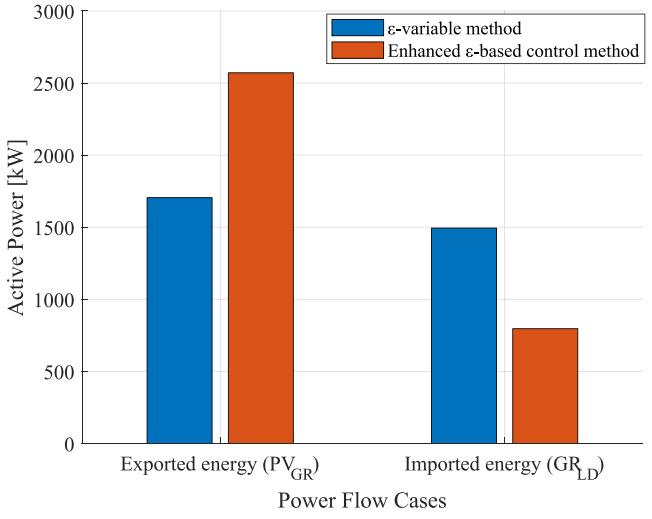

Fig. 10. The results for the standard ε-variables and optimal ε-variables for one year.

on grid-supplied energy. In addition, the increased exported energy demonstrates a substantial increase of approximately 50.8% in the use of RESs, emphasizing the enhanced integration of RESs into the MG system. From a cost perspective, the implementation of S-MPC yields substantial advantages. The decreased dependency on imported energy reduces the costs associated with grid-supplied electricity. While the specific cost reduction percentage can vary based on individual circumstances, the overall cost savings attributable to S-MPC-optimized control decisions are evident. In summary, the implementation of S-MPC demonstrates its effectiveness in optimizing the energy management system of the microgrid. This is evidenced by a significant reduction in energy imported from the grid, an impressive increase in the use of RESs, and the resulting cost savings. The application of S-MPC demonstrates its superiority to the ε-variables method, establishing it as a viable and advantageous strategy for improving the performance and sustainability of flexible hybrid MGs.

5.3. Use case 3: Incorporating plug-and-play EV fleet

We observe slight variations in the power profiles of EVs between the two controllers in Fig. 11. The logical Based-EMS Controller manages the EV fleet and distributes power based on predefined rules and heuristics. However, manual adjustments or modifications may be necessary when integrating new EVs into the system. The MPC Based-EMS Controller, on the other hand, leverages the plug-and-play capability of S-MPC to enable the seamless integration of new EVs into the system without extensive reconfiguration. As shown in Fig. 11, the MPC algorithm adapts to changes in the composition of the EV fleet and optimizes power distribution based on the current state of the system, taking into account factors such as EV load requirements, grid constraints, and forecasts. MPC Based-EMS Controller scalability and adaptability are enhanced by the plug-and-play capability of S-MPC. It simplifies the incorporation of new EVs into the fleet and ensures efficient utilization of their variable energy resources. This capability allows the controller to effectively manage the variability and unpredictability of the EV fleet, resulting in optimized power flows and enhanced system performance. In conclusion, the plug-and-play capability of S-MPC in the MPC Based-EMS Controller improves its adaptability and scalability, allowing for seamless integration of new EVs and efficient fleet management.

The SOAcc variables play a crucial role in the decision-making processes of the energy management system, allowing for the efficient utilization of energy resources. By monitoring and controlling SOAcc levels, the system can ensure optimal charging and discharging of the battery and EVs, thereby balancing supply and demand for energy. In Fig. 12, variations in SOAcc indicate the dynamic nature of the system's operation. The SOAcc of the EV fleet ($SOAcc_1^{EV}$, $SOAcc_2^{EV}$, and $SOAcc_3^{EV}$) are working at desired conditions because of our optimal method. These variations denote substantial modifications to the control strategy, such as switching between battery discharging and grid running modes or battery discharging and EV running modes. Overall, the SOAcc variables provide valuable information about the energy storage levels of the system's battery and EVs. Their fluctuations and patterns highlight the dynamic nature of the energy management system, which enables the efficient use of available energy resources and the effective adaptation to changing system conditions and control strategies.

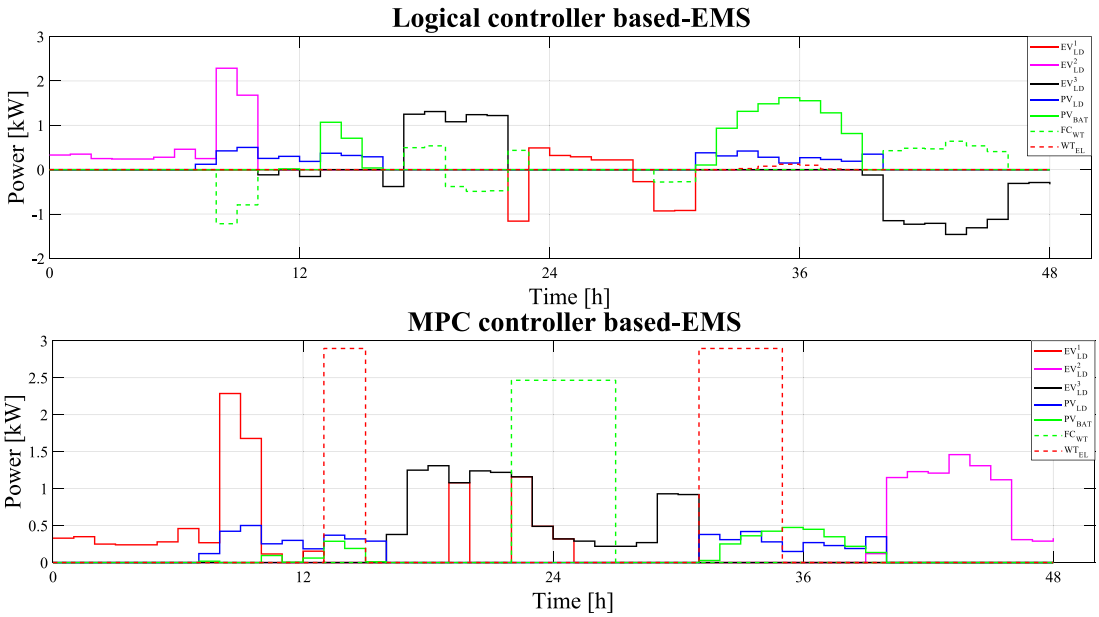

Fig. 11. Incorporating plug-and-play EV fleet using the logical controller and MPC controller based-EMS.

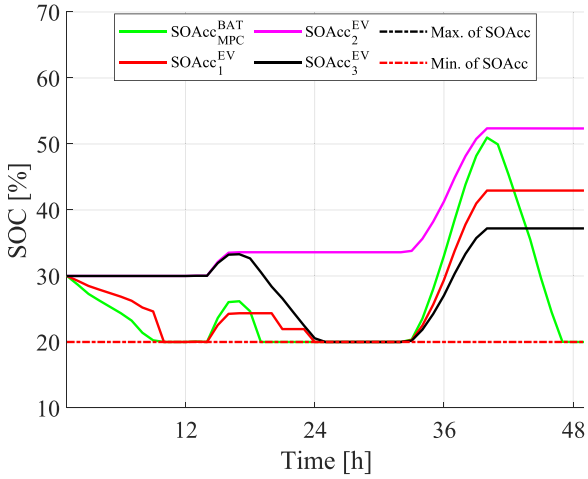

Fig. 12. The illustration of the SOAcc of the battery is the hybrid control method.

5.4. Use case 4: Islanded MG

Grid-Connected Mode: The results for grid-connected mode display the transition points (TPs) at specific time steps, indicating significant changes in system operation. In this mode, the TP indicates the transition from the battery (BAT) discharging to the GR operation, as well as the transition from BAT discharging to BAT charging. As shown in Fig. 13, at 12 h, 16 h, 22 h, and 25 h, the TP signifies the end of BAT charging and the start of GR running. This indicates that the battery has reached its capacity, and the system has switched to using grid power. The transition from BAT discharge to GR operation indicates the capacity limitations of the battery and the need to rely on the grid to meet the load requirements. In addition, the TP at 39 h indicates the end of BAT discharging and the beginning of BAT charging. This indicates that the battery is depleted and requires recharging, possibly in preparation for future grid instability or increased load demand. The transition from BAT discharging to BAT charging demonstrates the system's adaptability and capacity to optimize its operation by recharging the battery energy storage.

Islanded Mode: Similar TPs are observed in the islanded mode, indicating significant changes in system operation. The TP represents the transition from BAT discharge to GR operation and from BAT discharge to EV operation. As demonstrated in Fig. 13, the TPs at 12 h, 16 h, 22 h, and 25 h indicate the conclusion of BAT discharge and the start of GR running. This indicates that, in the absence of a grid connection, the battery has reached its minimum capacity, and the system switches to utilizing power from a nearby generator or renewable sources. In the islanded mode, the switch from BAT discharge to GR operation signifies the system's reliance on alternative power sources. In addition, the TP at 39 h indicates the end of BAT discharge and the beginning of EV operation. This indicates that the battery has been depleted, and the system has resorted to using power from EVs to meet load requirements. The transition from BAT discharge to EV operation exemplifies the system's flexibility and plug-and-play capability, allowing EVs to contribute to the power supply in islanded mode.

6. Conclusions

We conducted four case studies which demonstrate that the standard (non-optimal) ε-variables have several advantages, such as being scalable and practical for flexible hybrid MGs, especially complex hybrid power systems. However, ε-variables are not optimal. On the other hand, MPC predicts the system's future behavior and chooses the optimal control action using a mathematical model. At each time step, MPC solves an optimization problem using the system's current state, predicted future states, and a cost function that reflects performance objectives and constraints. Nevertheless, it cannot control the flexible hybrid MG because of multiple operating models. Based on the system's state and performance goals, S-MPC chooses a model and control strategy. However, S-MPC requires much more steps making it harder to implement. In order to cope with this issue, the decisions of S-MPC are translated into the ε-variables. By doing so, a systematic methodology is obtained, and the control structure is significantly simplified. In other words, this hybrid control method systematically and practically controls and supervises the complex hybrid MGs. Thus, it can permit more complex EMSs to be adopted readily. Our results indicate that the proposed controller synthesis method provides an efficient solution for optimally controlling flexible hybrid MGs with PnP capabilities by increasing the amount of energy export to the utility grid by 50.77%

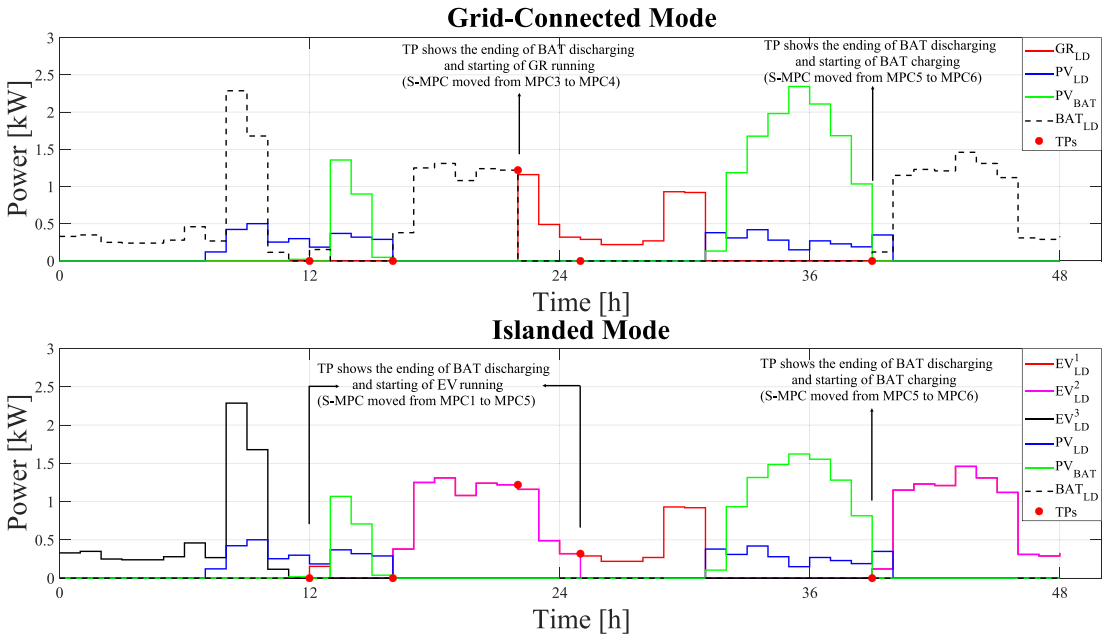

Fig. 13. The results of power flow when the MG is in grid-connected mode and islanded mode.

and subsequently reducing the amount of energy import from the grid by 46.7%. For future studies, the computational power of S-MPC can be decreased by eliminating the prediction horizon. By doing that, the steps of S-MPC can be reduced. This can be done by merging the S-MPC and one of the artificial neural network methods, such as recurrent neural networks and convolutional neural networks.

CRediT authorship contribution statement

Muhammed Cavus: Writing – review & editing, Writing – original draft, Visualization, Validation, Software, Methodology, Data curation, Conceptualization. **Adib Allahham:** Writing – review & editing, Writing – original draft, Visualization, Investigation, Data curation. **Kabita Adhikari:** Writing – review & editing, Supervision. **Damian Giaouris:** Writing – review & editing, Supervision.

Declaration of competing interest

The authors declare that they have no known competing financial interests or personal relationships that could have appeared to influence the work reported in this paper.

Data availability

Data will be made available on request.

Acknowledgement

This research was funded by the Turkish Ministry of National Education.

References

[1] Emad D, El-Hameed M, Yousef M, El-Fergany A. Computational methods for optimal planning of hybrid renewable microgrids: a comprehensive review and challenges. Arch Comput Methods Eng 2020;27:1297–319.
[2] Yoldaş Y, Önen A, Muyeen S, Vasilakos AV, Alan I. Enhancing smart grid with microgrids: Challenges and opportunities. Renew Sustain Energy Rev 2017;72:205–14.
[3] Ishaq S, Khan I, Rahman S, Hussain T, Iqbal A, Elavarasan RM. A review on recent developments in control and optimization of micro grids. Energy Rep 2022;8:4085–103.
[4] Nshuti HM. Centralized and decentralized control of microgrids. 2022.
[5] Herc L, Pfeifer A, Duić N, Wang F. Economic viability of flexibility options for smart energy systems with high penetration of renewable energy. Energy 2022;252:123739.
[6] Hirsch A, Parag Y, Guerrero J. Microgrids: A review of technologies, key drivers, and outstanding issues. Renew Sustain Energy Rev 2018;90:402–11.
[7] Veneri O. Technologies and applications for smart charging of electric and plug-in hybrid vehicles. Springer; 2017.
[8] Ravi SS, Aziz M. Utilization of electric vehicles for vehicle-to-grid services: Progress and perspectives. Energies 2022;15(2):589.
[9] Anthony Jnr B. Integrating electric vehicles to achieve sustainable energy as a service business model in smart cities. Front Sustain Cities 2021;3:685716.
[10] Sadabadi MS, Shafiee Q, Karimi A. Plug-and-play robust voltage control of DC microgrids. IEEE Trans Smart Grid 2017;9(6):6886–96.
[11] Nikkhah S, Allahham A, Bialek JW, Walker SL, Giaouris D, Papadopoulou S. Active participation of buildings in the energy networks: Dynamic/operational models and control challenges. Energies 2021;14(21):7220.
[12] Pamulapati T, Cavus M, Odigwe I, Allahham A, Walker S, Giaouris D. A review of microgrid energy management strategies from the energy trilemma perspective. Energies 2022;16(1):289.
[13] Silvente J, Kopanos GM, Dua V, Papageorgiou LG. A rolling horizon approach for optimal management of microgrids under stochastic uncertainty. Chem Eng Res Des 2018;131:293–317.
[14] Parisio A, Rikos E, Glielmo L. Stochastic model predictive control for economic/environmental operation management of microgrids: An experimental case study. J Process Control 2016;43:24–37.
[15] Cheng J, Duan D, Cheng X, Yang L, Cui S. Probabilistic microgrid energy management with interval predictions. Energies 2020;13(12):3116.
[16] Marín LG, Sumner M, Muñoz-Carpintero D, Köbrich D, Pholboon S, Sáez D, et al. Hierarchical energy management system for microgrid operation based on robust model predictive control. Energies 2019;12(23):4453.
[17] Nikkhah S, Allahham A, Royapoor M, Bialek JW, Giaouris D. A community-based building-to-building strategy for multi-objective energy management of residential microgrids. In: 2021 12th international renewable engineering conference. IEEE; 2021, p. 1–6.
[18] Nikkhah S, Allahham A, Royapoor M, Bialek JW, Giaouris D. Optimising building-to-building and building-for-grid services under uncertainty: A robust rolling horizon approach. IEEE Trans Smart Grid 2021;13(2):1453–67.
[19] Nawaz A, Wu J, Ye J, Dong Y, Long C. Distributed MPC-based energy scheduling for islanded multi-microgrid considering battery degradation and cyclic life deterioration. Appl Energy 2023;329:120168.
[20] Bordons C, Garcia-Torres F, Ridao MA. Model predictive control of microgrids, vol. 358, Springer; 2020.
[21] Fang X, Dong W, Wang Y, Yang Q. Multiple time-scale energy management strategy for a hydrogen-based multi-energy microgrid. Appl Energy 2022;328:120195.
[22] Allahham A, Alla H. Post and pre-initialized stopwatch Petri nets: Formal semantics and state space computation. Nonlinear Anal Hybrid Syst 2008;2(4):1175–86.

[23] Javaid CJ, Allahham A, Giaouris D, Blake S, Taylor P. Modelling of a virtual power plant using hybrid automata. J Eng 2019;2019(17):3918–22.
[24] Allahham A, Alla H. Monitoring of timed discrete events systems with interrupts. IEEE Trans Autom Sci Eng 2009;7(1):146–50.
[25] Pamulapati T, Allahham A, Walker SL, Giaouris D. Evolution Operator-based automata control approach for EMS in active buildings. IET; 2022.
[26] Khawaja Y, Allahham A, Giaouris D, Patsios C, Walker S, Qiqieh I. An integrated framework for sizing and energy management of hybrid energy systems using finite automata. Appl Energy 2019;250:257–72.
[27] Giaouris D, Papadopoulos AI, Ziogou C, Ipsakis D, Voutetakis S, Papadopoulou S, et al. Performance investigation of a hybrid renewable power generation and storage system using systemic power management models. Energy 2013;61:621–35.
[28] Cavus M, Allahham A, Adhikari K, Zangiabadia M, Giaouris D. Control of microgrids using an enhanced model predictive controller. PEMD 2022.
[29] Cavus M, Allahham A, Adhikari K, Zangiabadi M, Giaouris D. Energy management of grid-connected microgrids using an optimal systems approach. IEEE Access 2023.
[30] Zhu B, Tazvinga H, Xia X. Switched model predictive control for energy dispatching of a photovoltaic-diesel-battery hybrid power system. IEEE Trans Control Syst Technol 2014;23(3):1229–36.
[31] Maślak G, Orłowski P. Microgrid operation optimization using hybrid system modeling and switched model predictive control. Energies 2022;15(3):833.
[32] Giaouris D, Papadopoulos AI, Patsios C, Walker S, Ziogou C, Taylor P, et al. A systems approach for management of microgrids considering multiple energy carriers, stochastic loads, forecasting and demand side response. Appl Energy 2018;226:546–59.
[33] Li H, Zhao L. Data-driven distributionally robust joint chance-constrained optimization for industrial utility systems under uncertainty. In: Computer aided chemical engineering, vol. 52, Elsevier; 2023, p. 935–41.
[34] Wang L. Model predictive control system design and implementation using mATLAB®. Springer Science & Business Media; 2009.
[35] Cortés P, Kouro S, La Rocca B, Vargas R, Rodríguez J, León JI, et al. Guidelines for weighting factors design in model predictive control of power converters and drives. In: 2009 IEEE international conference on industrial technology. IEEE; 2009, p. 1–7.
[36] Makonin S. HUE: The hourly usage of energy dataset for buildings in British columbia. Data in Brief 2019;23.
[37] Ipsakis D, Voutetakis S, Seferlis P, Stergiopoulos F, Elmasides C. Power management strategies for a stand-alone power system using renewable energy sources and hydrogen storage. Int J Hydrogen Energy 2009;34(16):7081–95.